

Pressure-flow dynamics with semi-stable limit cycles in hydraulic cylinder circuits

Michael Ruderman¹, Stefan Kaltenbacher², Martin Horn³

Abstract—In hydraulic circuits of the standard fluid-power actuators and mechanisms, like the linear-stroke cylinders, some hydrodynamic effects are often neglected. It happens mainly due to their complexity and secondariness in comparison with the principal transient and steady-state behavior of the hydromechanical process variables, such as the differential pressure and relative displacement and its rate, in other words the piston stroke and velocity. However, a constrained motion of the cylinder piston can give rise to the back coupled excitation of the pressure-flow dynamics, especially upon mechanical impact at the cylinder limits. Following to that, semi-stable limit cycles can arise while the hydraulic cylinder remains under pressure without apparent displacement. This paper analyzes such back-coupled pressure-flow dynamics, derived from the partial differential momentum equation with involvement of Darcy-Weisbach hydraulic damping and continuity equation, out from which the closed-form system dynamics is formulated. In both, simulations and laboratory experiments, it is shown that if a constrained motion applies, the solution diverges from steady-state and can develop to the behavior similar to a semi-stable limit cycle.

I. INTRODUCTION

Hydrodynamic principles and properties, see e.g. [1], [2] for basics, and the derived (from it) behavior of the system state variables are essential for analysis, modeling, and control of hydromechanical actuators and machines. While more sophisticated considerations of the single principal components, like for example proportional- and servo-valves, can be found also in the system and control literature, see e.g. [3], the whole hydro-mechanical response of the corresponding controlled mechatronic plant is often captured by the simplified dynamic models. Several transient and characteristic (often nonlinear) properties are neglected or reduced as for the order and couplings between the state variables. A typical modeling procedure, see e.g. [4], considers the nonlinear orifice equations but the first-order hydrodynamics result solely from the continuity equations. Such modeling approaches are considered sufficiently, also for more advanced controls of the hydro-mechanical systems such as, for example, linear parameter varying (LPV) [5] or sliding-mode based [6]. An experimental evaluation of different (position) control methods for the hydraulic systems can be found e.g. in [7]. It can also be noticed that the complex coupled hydro-mechanical dynamics and the hardware assemblies bear general difficulties for an access and knowledge about

internal states, so that various estimation and observation techniques remain further on in focus of the recent research, see e.g. [8]. Even a simplified consideration of the whole hydro-mechanical system, like a classical valved-controlled hydraulic cylinder, discloses several sophisticated transfer characteristics when changing the linearization points and operation ranges, see e.g. [9].

When a constrained motion, like in case of reaching the cylinder limits or other boundary conditions apply, the coupled hydro-mechanical dynamics give rise to several, often undesired, effects in the transient and/or stationary response of the fluid powered system. One of those, which is the objective of this communication, is a possible appearance of semi-stable limit cycles at the constant supply pressure, after the relative displacement of the cylinder piston becomes constrained. This, at first glance not self-evident, phenomenon can have practical relevance for the hydraulic actuators where the coupled pressure-flow dynamics is not explicitly attenuated, correspondingly counterbalanced, by the dedicated auxiliary hardware integrated into hydraulic circuits. Taking into account the flow dynamics in pipes and considering, this way, the inlet and outlet flow as process state variables, the order of hydrodynamics is increased. Based on a most simple lumped parameters modeling, without analyzing a wave propagation in the hydraulic medium, the pressure-flow hydrodynamics is shown to exhibit long-term oscillations and, eventually, semi-stable limit cycles.

The rest of the paper is organized as follows. The basic notations and preliminaries required for reading are provided in section II. The overall modeling of the system under consideration is described in section III. In section IV, we show the pressure-flow dynamic response within numerical simulation, while an experimental case study is exemplary given in section V. The paper is concluded by section VI.

II. NOTATION AND PRELIMINARIES

Unless otherwise stated, all state variable and signals are with SI units. The time argument (t) will be sometimes omitted, for the sake of simplicity, while the time units are also abbreviated by 'sec'. The derivative operator is written d , meaning dy/dx is the derivative of y with respect to x .

Several hydro-mechanical process parameters are assumed to be constant. Those are the hydraulic oil density ρ , upper bound of the bulk modulus E_{\max} , and the Darcy-Weisbach [2] friction factor λ . The internal leakage coefficient of cylinder, which characterizes an additional pressure drop due to partial (minor) penetration of the hydraulic medium between both chambers, is neglected i.e. assumed to be zero.

¹M Ruderman is with University of Agder (UiA) Norway, email: michael.ruderman@uia.no

²S Kaltenbacher was with Institute of Automation and Control at Graz University of Technology, Austria

³M Horn is with Graz University of Technology, Austria, email: martin.horn@tugraz.at

The volumetric flow of the inlet and outlet hydraulic circuit is subject to continuity equations (see below in section III-A), meaning the total hydraulic volume of cylinder and piping remains constant. The constrained relative displacement of the cylinder piston has one translational degree of freedom, and the motion dynamics is with lumped parameters of the solid moving mass and total frictional damping. The hydraulic medium in the pipes and cylinder chambers complies with Darcy-Weisbach theory [10]. The subindex $i = \{A, B\}$ will be used for both, the inlet and outlet piping and, respectively, chambers of the connected hydraulic cylinder.

All parameter values used for the numerical simulations are given in section IV, while the experimental case study is provided qualitatively, that without exact identification or fit of the residual parameter values.

III. MODELING

A. Pressure-flow dynamics

The volumetric flow rate Q and pressure P are described separately for both sides of the powered hydraulic cylinder. The external interface is considered to be on the supply inlet (denoted by the subindex s) and outlet to tank (denoted by the subindex t). Assuming the inlet pressure P_s and outlet pressure P_t , the flow dynamics is obtained from the partial differential momentum equation [2] as

$$l_i(gA_i)^{-1} \frac{d}{dt} Q_i(t) = (g\rho)^{-1} \Delta P_i(t) - H(Q_i(t)). \quad (1)$$

The pressure difference on the interface is given by $\Delta P_A = P_s - P_A$ and $\Delta P_B = P_B - P_t$ correspondingly. The involved physical parameters, assumed to be known, are the gravitational acceleration constant g , the length l_i and cross section area A_i of the pipes, and the hydraulic fluid density ρ . The flow-dependent hydraulic damping $H(\cdot)$ is captured by the Darcy-Weisbach equation, see below in section III-B. It should be noted that the lumped parameters modeling approach, without involvement of partial differential equations, assumes the same pressure gradient at all locations in the piping as on the chambers' port of the hydraulic cylinder. Correspondingly, the dynamic state variables of the volumetric flow rate distinguish only for the corresponding ports A and B , while zero leakage is assumed for all elements of the hydraulic circuits.

For deriving the pressure dynamics, one considers the flow of a slightly compressible fluid within a conduit having rigid (to say inelastic) walls. The control volume may then shorten or elongate as the pressure changes. The pressure dynamics is determined by the volumetric flow rate, on the one hand, and by the varying volume rate governed by the piston displacement, on the other hand. The resulted pressure gradient, obtained from the continuity equation with respect to the moving mechanical piston of the hydraulic cylinder without leakage, is then given by

$$\frac{d}{dt} P_i(t) = -E(P_i(t)) (X_i(t) B_i)^{-1} \left(Q_i(t) + B_i \frac{d}{dt} x(t) \right). \quad (2)$$

Here the effective cross section, on both sides of the cylinder's piston, is denoted by B_i . It is worth noting that for an asymmetric, due to the one-side rod, hydraulic cylinder (like one we are considering in the recent study) the cross sections $B_A \neq B_B$ are largely different. The corresponding dynamic state of the control volume, associated with both chambers, is given by $X_A = x - L$ and $X_B = x$, while the relative displacement variable of the moving piston is $0 \leq x \leq L$. Further it should be stressed that the control volume $(L - x)B_A$ and $x B_B$, of the left and right chamber respectively, would become zero at the boundary conditions and, therefore, would cause singularities in the solution of the pressure dynamics (2). Therefore, a biased length variable $x + \alpha$, with $\alpha = \text{const} > 0$, is used instead of x when computing the X_i state. Note that this is in accord with the continuity equation (2), since a non-zero volume is still present in each piping line even when the corresponding cylinder's chamber becomes empty. The compressibility-inverse bulk modulus of the hydraulic circuits, given by

$$E(P) = c_1 E_{\max} \log \left(c_2 \frac{P}{P_{\max}} + c_3 \right), \quad (3)$$

is considered as a function of the pressure state and parameters $c_1, c_2, c_3, E_{\max}, P_{\max}$. This is according to the known modeling approaches to be found in the applied hydrodynamics literature, cf. e.g. [1].

B. Darcy-Weisbach equation

The well established Darcy-Weisbach formula, cf. [10],

$$H(Q) = \lambda_i |Q| Q, \quad (4)$$

with constant friction factor λ_i is applied to express head losses at fittings, valve inlet and outlet points of the hydraulic set-up. This type of friction is usually known to be part of "minor losses", a term broadly used in literature [11]. These pipe contractions typically lead to local turbulence, and subsequently to appropriate pressure or head losses. As the considered pipe lengths are in the range of 1 m only, hydraulic friction due to pipe roughness does play a subordinate role in comparison to these minor losses and are thus neglected.

C. Motion behavior

The motion dynamics of the cylinder piston, with the lumped mass m and resistive kinetic friction force F , is captured by

$$m \frac{d^2}{dt^2} x(t) = -P_A(t) B_A + P_B(t) B_B - F \left(\frac{d}{dt} x(t) \right). \quad (5)$$

We notice that no additional external load force is included here and the piston is free to move, with one translational degree of freedom, until it hits either of both cylinder caps. The motion dynamics (5) describes the unconstrained relative displacement, while its boundary conditions at $x = 0 \vee L$ are captured as given below in section III-D. The overall mechanical friction, mainly due to the contacts between the piston rod and lip seal, and between the piston o-rings, seals

and cylinder, is described by a linear combination of the viscous and Coulomb friction force. This can be written as

$$F\left(\frac{d}{dt}x(t)\right) = c_4 \frac{d}{dt}x(t) + c_5 \tanh\left(c_6 \frac{d}{dt}x(t)\right), \quad (6)$$

where the viscous and Coulomb friction coefficients are c_4 and c_5 correspondingly. The principal shape of the static

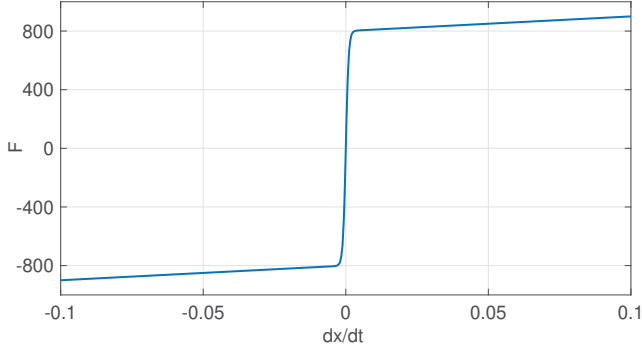


Fig. 1. Principal shape of the viscous and Coulomb friction force (6).

velocity-force map of the viscous and Coulomb friction (6) is exemplary shown in Fig. 1, here without units and specific parameter values. Note that in order to avoid discontinuity at the velocity zero crossing, a hyperbolic tangent function is assumed (instead of the sign) in (6). Here an approximative scaling factor c_6 is used for approaching discontinuity at zero-crossing. Such approximative description is justified and widely used in multiple hydro-mechanical studies, see e.g. [1] and references therein.

D. "Bouncing ball" impact

When the piston hits the cylinder wall, at both stroke limits, an unconstrained motion terminates and the state integration $x = \int \dot{x}dt$ has to be bounded. More important appears the handling of the relative velocity $\dot{x} = \int \ddot{x}dt$. The integrator state is then reset to

$$\dot{x}^+ = -\beta\dot{x}(t_i), \quad (7)$$

where \dot{x}^+ is the successor velocity state immediately upon the impact at t_i . The restitution coefficient, see e.g. [12], $\beta = 1/2$ is assigned to avoid the fully elastic impact and, this way, to allow for sufficient structural damping by the cylinder barrel and cap. Note that the assumed relatively low β -value allows avoiding spurious oscillations upon an impact, which is relevant for a low-inertial and highly damped hydromechanical system. The resulted relative motion during the (partially elastic) impacts is also known as "bouncing ball" effect, as exemplary shown in Fig. 2 for $x(t)$ after the impact and until the motion stops. Here the displacement is unitless and without particular parameter values.

IV. NUMERICAL SIMULATION

Numerical simulation of the model (1)-(7) is realized in the Simulink environment with a variable-step solver. The latter is explicitly required due to fast-slow dynamics of the whole system (1)-(6) and for accurately handling the

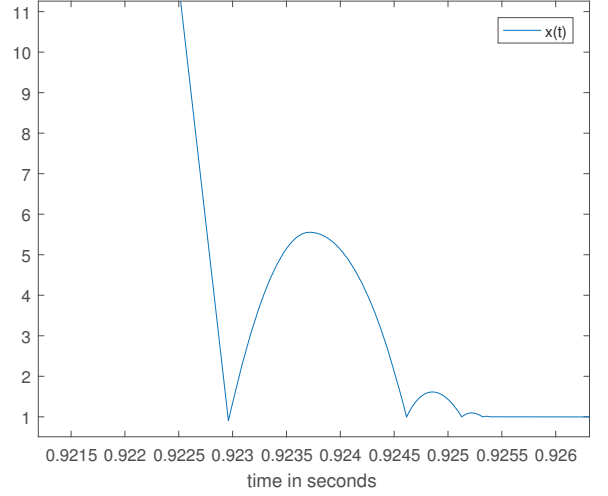


Fig. 2. Example of relative piston displacement $x(t)$ upon the impact.

reset conditions, like during a "bouncing ball" impact. The supply pressure P_s is assigned to be of the same principal shape, yet without oscillations, as the P_{PRV} measured within the experimental case study, cf. Fig. 6. The assigned model parameters are listed in Table I. Note that the parameters are selected to be largely in accord with the experimental setup, while several of them, which are not available, have been assumed from hydraulic literature.

TABLE I
NUMERICAL SIMULATION PARAMETERS.

Variable	Units	Description
x	m	piston position
P_i	Pa	pressure in chamber
Q_i	m ³ /s	volumetric flow rate
P_s	Pa	supply pressure (after PRV)
$P_t = 0$	Pa	pressure in tank
$m = 20$	kg	lumped mass (piston and load)
$L = 0.2$	m	length of hydraulic cylinder
$B_A = 0.02^2\pi$	m ²	cross section area chamber A
$B_B = (0.02^2 - 0.0125^2)\pi$	m ²	cross section area chamber B
$A_i = 0.0035^2\pi$	m ²	cross section area of pipes
$c_6 = 10^5$	-	scaling for static friction
$c_4 = 700$	kg/s	friction coefficient
$c_5 = 800$	kg/s	friction coefficient
$\lambda_A = 8.0409 \times 10^7$	s/m ⁵	Darcy-Weisbach factor
$\lambda_B = 1.6555 \times 10^9$	s/m ⁵	Darcy-Weisbach factor
$g = 9.81$	m/s ²	gravitational acceleration
$\rho = 0.88 \times 10^3$	kg/m ³	hydraulic oil density
$\ell_A = 1$	m	pipe length port A
$\ell_B = 2$	m	pipe length port B

The simulated response of the pressure in the left and right chambers of the hydraulic cylinder are shown opposite to each other in Fig. 3. After transient response, the chambers pressure behave constant, as expected, during the steady-

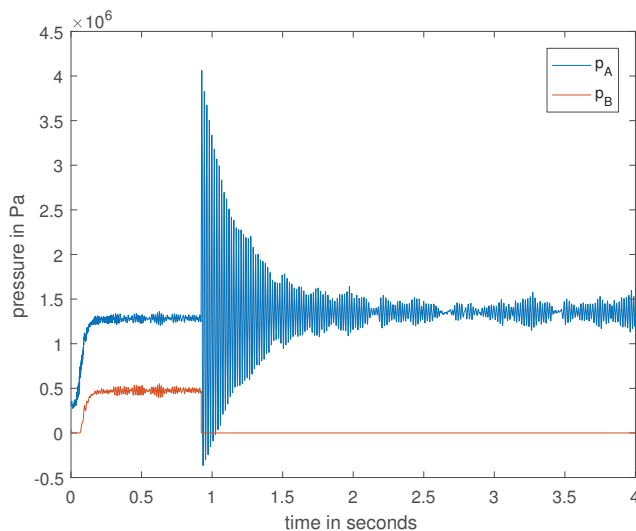


Fig. 3. Simulated pressure response in the left and right chambers.

state motion of the cylinder piston, that until the time instant around 0.92 sec. Afterwards, the piston hits the cylinder cap, and the pressure P_A of the powered chamber undergoes a large excitation, leading immediately to an oscillating pattern. Note that in the following, we focus on the hydraulic dynamic quantities (pressure and flow) only, since the relative displacement state is not measured in our system setting. It is worth noting that the resulting frequency of the P_A oscillations is approximately twice as high as the one recorded in the measurements. However, when reducing, for instance, the bulk modulus parameter, the frequency could be adjusted to the one observed in the measurements. A possible reason for that could be entrapped air in the hydraulic setup. One can recognize that the pressure oscillations can be well reconstructed, cf. Fig. 3, for the bounded motion at the constant supply pressure. The pressure oscillations subsequently cause oscillations in the volumetric flow rate Q_A , see Fig. 4, according to the coupled hydrodynamics (1), (3). An irregular pattern of the residual oscillations, at times larger than 2 sec, indicates a persistent excitation of the hydrodynamics which can cause appearance of the semi-stable limit cycles. Furthermore, from (1)-(4), it becomes apparent that the way of modeling and parameterizing the bulk modulus and hydraulic friction bear the most uncertainties in describing the hydrodynamic behavior. Since both appear as the state-varying quantities equivalent to the stiffness and damping factors of an oscillator, it comes as not surprising that the oscillating response is nonlinear and non-trivial. For continuous energizing, by a constant supply pressure, an emerge of the semi-stable limit cycles seems theoretically possible.

V. EXPERIMENTAL CASE STUDY

The following experimental case is recorded on the hydraulic setup (see Fig. 6) which includes a standard linear-stroke cylinder. The latter is separated into the left and right chamber (denoted by A and B) by the moving one-side

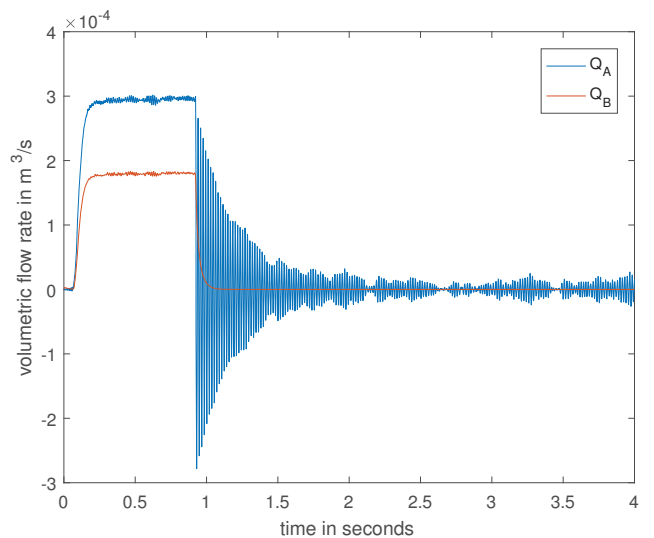


Fig. 4. Simulated flow rate response in the left and right chambers.

piston with the seal. A sufficiently high pressure difference between the chambers causes the piston to move. An unidirectional motion, from the left to the right, with successive hitting the cylinder limit is considered, so that P_A pressure only is of prime interest. Pressure P_B is also considered for showing the difference between the unconstrained motion phase and the limiting case where P_B is around zero as the B -chamber becomes unpressurized. The bi-directional control valve (BDCV) was not actuated and remained fully open during the experiments. Effectively, the BDCV only increases the hydraulic friction by a narrowing of the pipes connected to both of the cylinder's chambers.

The Pressure Reduction Valve (PRV) is located between the pressure supplying line and BDCV. It is worth noting that PRV is open-loop controlled and can be actuated to regulate the pressure reduction prior to BDCV. The return connection pipe of BDCV, for outlet of the low pressure, leads to the tank which is filled with hydraulic fluid. The pressure sensors are directly installed on the piping connected to the chambers A and B , and at the output of PRV, i.e. the latter is measuring the reduced pressure in the piping between PRV and BDCV. No relative displacement measurements of the moving cylinder are available. Some further details on the experimental setup can also be found in [8].

Case description: Supplying a nearly constant pressure (see Fig. 6 until $t \approx 1.1$ sec) causes the piston to move from the left to the right until it hits the cylinder cap. At that instant, strong oscillations in the pressure occur, see Fig. 7, which resemble a limit cycle. It should be noted that the transfer characteristics of PRV and its dynamic behavior self where not a part of this investigation. Here one can notice, from Fig. 6, that the supply pressure behind the PRV, i.e. the measured P_{PRV} , exhibits also strong oscillations after the piston motion becomes constrained, while the supply pressure input to PRV remained nearly constant. Therefore, it is suspected that the back-propagated pressure-flow dynamics

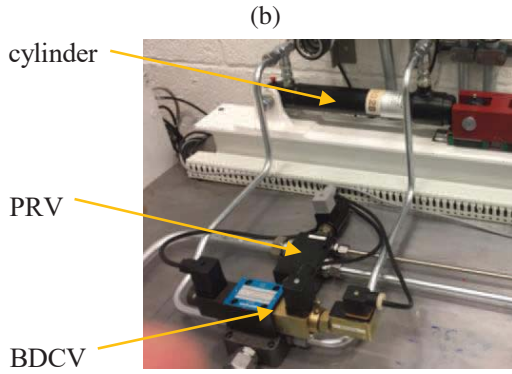
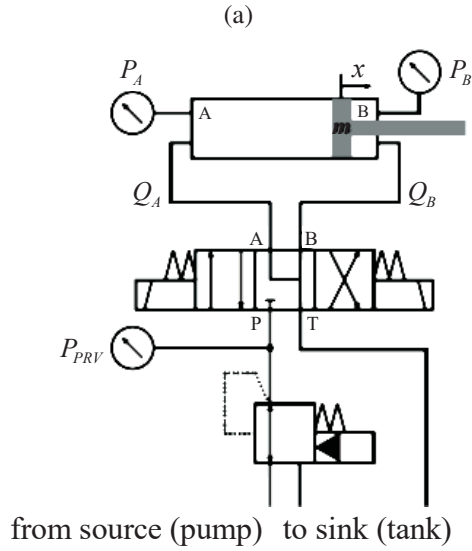


Fig. 5. Schematic representation of the hydraulic circuit (a), and laboratory view of the experimental setup (b).

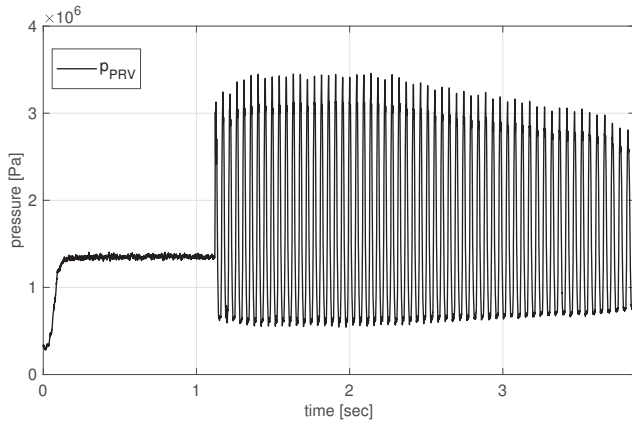


Fig. 6. Measured PRV outlet pressure P_{PRV} during the experiments.

with high transient oscillations upon the impact additionally excited the disturbing oscillations own to the PRV self. Still, the excited and continuously oscillating pressure-flow dynamics of hydraulic medium in the cylinders' connection can appear as a source (in addition to PRV) of the semi-stable limit cycles, cf. Fig. 7.

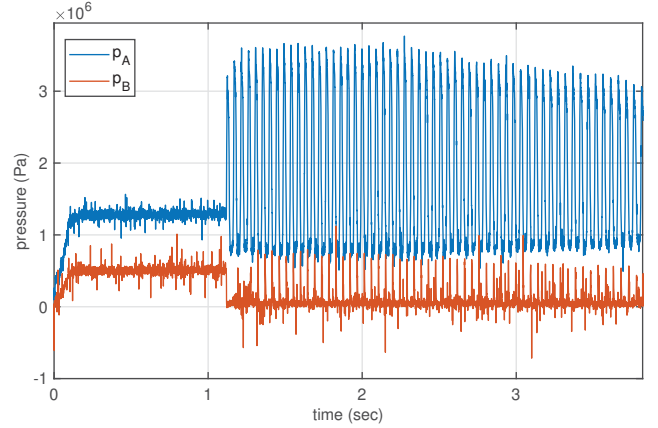


Fig. 7. Measured chambers' pressure P_A and P_B during unconstrained motion at $0 < t < 1.1$ sec and after hitting cylinder cap $t > 1.1$ sec.

Discussion: Several discussion points remain open regarding the above experimental case study. It would have been interesting to see whether the pressure oscillations do also cause continuous, even minor, displacements of the piston. Here the numerical simulation study, cf. sections III and IV, disclosed that displacement oscillations are quickly dying out, i.e. within several periods, even when the restitution coefficient is not close to zero and a partially elastic impact (which is less realistic for the cylinder caps) is assumed. Another open question directly relates to the PRV transfer behavior and the back-propagated oscillations or even amplified through it. Comparing the chambers' pressure response from the numerical and experimental studies, it is obvious that the simulated oscillations are converging faster and, to say, with a more 'exponential' shape. Still, it remains unclear how far the hydrodynamic damping and pressure-flow relationship can be accurately captured by the lumped parameters model, cf. section III. An 'ideal' PRV with less oscillating outlet pressure and additional flow sensing could bring more light into investigation of these issues.

VI. CONCLUSIONS

This paper addressed appearance of the slow-converging oscillations, and an associated semi-stable limit cycle, in the pressure-flow dynamics of the hydraulic circuit powering the linear-stroke cylinder which is subject to a constrained motion. The order of the hydrodynamic model has been increased by two, compared to a more frequently assumed first-order behavior of the continuity equations. As a result, the two-way coupled pressure-flow dynamics appear to be excited, and then long-term oscillating for boundary conditions of the mechanical displacement, i.e. once the moving piston of hydraulic cylinder hits the cylinder cap and remains in idle state. By means of a numerical simulation and an experimental case study, it has been demonstrated that the hydraulic medium can undergo complex dynamic behavior at constant supply pressure of the source and zero velocity of the mechanical load.

ACKNOWLEDGMENT

This work has received funding from the European Union Horizon 2020 research and innovation programme H2020-MSCA-RISE-2016 under the grant agreement No 734832.

REFERENCES

- [1] M. Jelali and A. Kroll, *Hydraulic servo-systems: modelling, identification and control*. Springer, 2012.
- [2] M. H. Chaudhry, *Applied Hydraulic Transients*. Springer, 2013.
- [3] B. Eryilmaz and B. H. Wilson, "Unified modeling and analysis of a proportional valve," *Journal of the Franklin Institute*, vol. 343, no. 1, pp. 48–68, 2006.
- [4] G. A. Sohl and J. E. Bobrow, "Experiments and simulations on the nonlinear control of a hydraulic servosystem," *IEEE transactions on control systems technology*, vol. 7, no. 2, pp. 238–247, 1999.
- [5] F. Wijnheijmer, G. Naus, W. Post, M. Steinbuch, and P. Teerhuis, "Modelling and LPV control of an electro-hydraulic servo system," in *IEEE Int. Conf. on Control Applications*, 2006, pp. 3116–3121.
- [6] S. Koch and M. Reichhartinger, "Observer-based sliding mode control of hydraulic cylinders in the presence of unknown load forces," *Elektrotechnik und Informationstechnik*, vol. 133, pp. 253–260, 2016.
- [7] A. Bonchis, P. I. Corke, and D. C. Rye, "Experimental evaluation of position control methods for hydraulic systems," *IEEE Transactions on Control Systems Technology*, vol. 10, no. 6, pp. 876–882, 2002.
- [8] M. Ruderman, L. Fridman, and P. Pasolli, "Virtual sensing of load forces in hydraulic actuators using second- and higher-order sliding modes," *Control Engineering Practice*, vol. 92, no. 104151, 2019.
- [9] M. Ruderman, "Full-and reduced-order model of hydraulic cylinder for motion control," in *IEEE Annual Conference of the Industrial Electronics Society (IECON)*, 2017, pp. 7275–7280.
- [10] G. O. Brown, "The history of the darcy-weisbach equation for pipe flow resistance," in *Environmental and Water Resources History*, 2003, pp. 34–43.
- [11] T. M. Walski, D. V. Chase, D. A. Savic, W. Grayman, S. Beckwith, and E. Koelle, "Advanced water distribution modeling and management," 2003.
- [12] A. Kharaz and D. Gorham, "A study of the restitution coefficient in elastic-plastic impact," *Philosophical Magazine Letters*, vol. 80, no. 8, pp. 549–559, 2000.